JAERI 1103

# $^{148}$Pm as a Primary Product of Thermal Neutron Fission of $^{233}$U and $^{235}$U

Feb. 1966

日本原子力研究所

Japan Atomic Energy Research Institute

JAERI 1103

UDC 681.142.01 : 007.3

# $^{148}$Pm as a Primary Product of Thermal Neutron Fission of $^{233}$U and $^{235}$U

## Summary

It was intended to determine the independent fission yields of $^{148m}$Pm and $^{148g}$Pm in the thermal neutron fission of $^{235}$U and $^{233}$U. The contribution of the $^{147}$Pm (n, $\gamma$) $^{148}$Pm reaction, which also occurs as the secondary reaction, was experimentally corrected by means of the simultaneous irradiation of a neodymium target and a uranium target. The fission yields of $^{148}$Pm could not be determined, but only their upper limits were estimated. These values are too small by a factor of 5 for $^{235}$U and 50 for $^{233}$U, compared with the values expected from the present systematics of nuclear charge distribution in fission.

Dec. 1965

Hirokazu Umezawa
Division of Research, Tokai Research Establishment
Japan Atomic Energy Research Institute

# $^{233}$U および $^{235}$U の熱中性子核分裂の一次生成物としての $^{148}$Pm

## 要　　旨

$^{233}$U と $^{235}$U の熱中性子核分裂における $^{148m}$Pm と $^{148g}$Pm の独立収率を測定することを試みた.

$^{148}$Pm は，核分裂生成物のひとつである $^{147}$Pm が再び中性子を捕獲することによっても生成する．この寄与はウラン試料とネオジム試料を共に同一条件で照射することによって実験的に補正した.

結果として，$^{148}$Pm の独立収率の値を決めることはできなかったが，その上限値を推定した．この上限値は現在の核分裂における核電荷分布の定説から予想される値より小さく，予想される最小値に比較して，$^{235}$U で 1/5，$^{233}$U の場合には 1/50 であった.

1965 年 12 月

日本原子力研究所，東海研究所
研究部，燃料化学研究室
梅 沢　弘 一

## Contents



## 目　　次

## 1. Introduction

Most nuclides of the fission products are unstable for $\beta$-dacay and consequently constitute $\beta$-decay chains of the fission products. Some of the nuclides, however, which have the stable precursors, are shielded against the $\beta$-decay chains and hence called shielded nuclides. The measurements of such shielded nuclides may represent the direct results of fission if the contribution of the secondary nuclear reactions is carefully removed.

$^{148}$Pm is one of the shielded nuclides and it is interesting to measure its fission yield from the following two points of view.

First, it has been concluded in the present systematics of nuclear charge distribution in low energy fission[1,2] that the fractional independent yield of the fragment with nuclear charge $Z$ is given by Eq. (1) for a given mass number A.

$$Y_A(Z) = (c\pi)^{-1/2} \exp\left[\frac{-(Z-Z_p)^2}{c}\right] \quad (1)$$

where $c$ is an empirical constant, $0.94 \pm 0.15$, and $Z_p$ is the most probable charge for the primary fission products of mass number A and is obtained from the Wahl's empirical $Z_p$ function[1]. An equal charge displacement hypothesis[3] also gives the similar $Z_p$ values. The systematics, however, have been based on the independent fission yields of the fission products which are rather located in the peak region of the mass-yield curve. Therefore it should be confirmed whether the above mentioned rules are valied for the fission products generated from the more asymmentric or symmetric fragmentation.

Second, two isomers of $^{148}$Pm are identified at present. They are $^{148g}$Pm with the spin of 1 and the half-life of $5.4\,d$ and $^{148m}$Pm with the spin of 6 and the half-life of $43\,d$[4,5]. The mean intrinsic angular momentum of the fragment is deducible from the independent yield ratio of the isomeric pair by calculations[6,7] based on a statistical theory and may be compared with the results reported for $^{81}$Se, $^{83}$Se[8], $^{131}$Te, and $^{133}$Te[9].

Cook[10] determined the upper limit of the fractional independent yield of $^{148g}$Pm in thermal neutron fission of $^{235}$U to be $1\times10^{-4}$, but any other results have not been reported concerning either the yield of $^{148g}$Pm or $^{148m}$Pm in the low energy fission. According to the systematics mentioned above, the fractional independent yields of $^{148}$Pm are expected to be $1\times10^{-4}$ for $^{235}$U and $1\times10^{-3}$ for $^{233}$U.

In this work it was intended to determine the independent yields of $^{148m}$Pm and $^{148g}$Pm in the thermal neutron fission of $^{235}$U and $^{233}$U. Especially $^{233}$U fission was expected to be quite a promising case for this purpose. In order to determine the independent fission yield of $^{148}$Pm it is important to remove the contribution of $^{147}$Pm (n, $\gamma$) $^{148}$Pm as the secondary nuclear reaction, since the fairly large cross section value[11] has been reported for the reaction and, besides, $^{147}$Pm is not the shielded nuclide. The correction for this contribution was made experimentally by means of the simultaneous irradiation of a neodymium target and a uranium target.

## 2. Experimental procedure

### 2.1 Target preparation and irradiation

$^{233}$U was purified by an anion exchange method. $^{233}$U adsorbed on a resin column was washed with 6 N HCl and eluted with 0.1 N HCl. Then it was electrodeposited on a copper foil from 0.2 M $HClO_4$ − 0.15 M $NH_4COOH$ solution using a platinum wire as the anode[12]. The thickness of the target was 0.2 − 0.3 mg of $^{233}$U/cm$^2$.

Uranium used for the $^{225}$U target had an isotopic composition of 0.67% $^{235}$U. It was purified by ethylether extraction, precipitated as oxalate, and ignited to $U_3O_8$. Uranium oxide was deposited on a copper foil by electromigrat ionfrom acetone with a mean thickness of 50—150 mg of U/cm$^2$.

Specpure grade neodymium oxide, from Johnson Matthey Co. Ltd., was deposited on a copper foil by electromigration with a mean thickness of 5—15 mg of Nd/cm$^2$. The neodymium was of natural isotopic composition. The contents of samarium and europium in the neodymium target material were determined to be 30 ppm and 3 ppm, respectively, by activation analysis. Also tested was the presence of any promethium in the neodymium oxide. The promethium fraction was extracted from unirradiated neodymium oxide of 100 mg and measured by a $2\pi$-type proportional counter. No $\beta$-activity was detected.

A cobalt foil prepared by electroplating with a thickness of $\sim$2 mg/cm$^2$ was used as a thermal neutron flux monitor. Metal pellets of iron and nickel were used to measure the fast neutron flux.

A uranium and a neodymium target wrapped in copper foil were again wrapped in aluminum foil to prevent cross contamination from each other, and they were enclosed in a quarz ampoule together with the neutron flux monitors. The targets were irradiated at the lowest position of the VT-5 irradiation hole of JRR-2 reactor for 60 to 130 hours. The thermal neutron flux at the position was $1.0\times10^{13}$ neutron/cm$^2$sec and the cadmium ratio was 230 for $^{60}$Co activity with the cadmium cover 1 mm thick. The fast neutron flux was of the order of $10^9$ neutron/cm$^2$sec when it was assumed to show the fission neutron spectrum.

## 2.2 Chemical separation

The uranium target was dissolved in 10 N nitric acid containing 1 mg each of neodymium and cesium as the carriers to prevent the adsorption in the glass wall. The nitrates were converted to the chlorides by repeating evaporation with 12 N hydrochloric acid and finally dissolved in 12 N hydrochloric acid. The solution was passed through a Diaion SA #100 anion-exchange resin column to remove uranium, copper, and the anionic fission products. The eluate, containing alkali metal, alkali earth, and rare earth elements, was made 0.1—0.5 N in acidity and adsorbed on a Diaion SK #1 cation exchange resin column. After washing the column with 0.1 N oxalic acid to remove the contaminations of zirconium and niobium, cesium was eluted with 1 N hydrochloric acid and the rare earth elements were eluted with a mixture of 2 portions of 0.25 M citric acid and 3 portions of 0.25 M diammonium citrate. The rare earth fraction was made acidic with an equivalent amount of hydrochloric acid and passed through another long cation exchange resin column to adsorb the rare earth elements. Promethium was separated from other rare earth elements by elution with a mixture of 7 portions of 0.5 M $\alpha$-hydroxyisobutylic acid and 3 portions of ammonium $\alpha$-hydroxyisobutylate. Just after promethium had been eluted completely, the eluant was switched to a mixture of 7 portions of 0.25 M citric acid and 3 portions of 0.25 M diammonium citrate to elute neodymium preferentially from the remaining rare earths. The fractions of promethium and neodymium were made acidic with an equivalent amount of hydrochloric acid, diluted with an equal amount of water, and each of them was passed through a small cation exchange resin column.

Promethium and neodymium concentrated on each column were eluted with 6 N hydrochloric acid after the ammonium ions were washed out with 2 N hydrochloric acid. Further purification of promethium was carried out by repeating the cation exchange process with $\alpha$-hydroxyisobutylate.

The procedure for the neodymium target was similar to that for the uranium target except the second ion exchange step which was not necessary for this target.

The cobalt monitor foil was dissolved in hydrochloric acid together with the aluminium cover. The cobalt was adsorbed on an anion exchange resin column with 10 N hydrochloric acid and eluted with 2 N hydrochloric acid. $^{54}$Mn was separated from iron by anion exchange using hydrochloric acid. Chemical treatment was not required for the nickel pellet.

It was confirmed that the chemical yields of the elements separated were more than 99% for the over-all procedure.

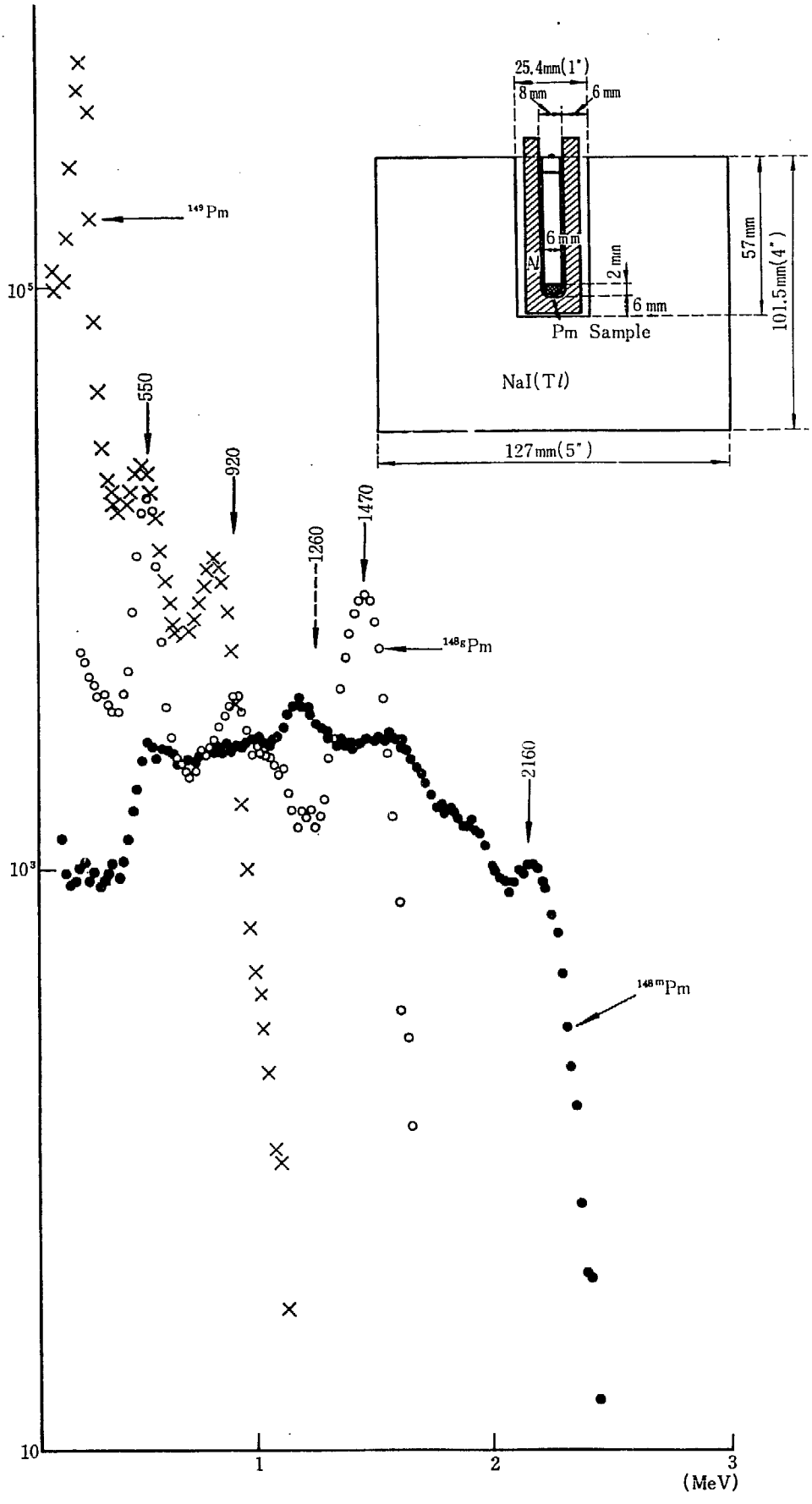
25.4mm(1")
8mm
6mm
6mm
Al
2mm
6mm
57mm
101.5mm(4")
Pm Sample
NaI(Tl)
127mm(5")
$^{149}$Pm
550
920
1260
1470
$^{148g}$Pm
2160
$^{148m}$Pm
$10^5$
$10^3$
10
1
2
3
(MeV)

Fig. 1

## 2.3 Radioactivity measurement

The activities of $^{148m}$Pm, $^{148g}$Pm, $^{147}$Nd, and $^{137}$Cs were measured, respectively. As for the monitors, $^{60}$Co, $^{58}$Co, and $^{54}$Mn were also determined.

The solution of promethium was transfered to a small polyethylene tube with inside diameter 6 mm and precipitated to the bottom by adding neodymium carrier of 0.5 mg and ammonium hydroxide. As regards the other samples, an appropriate portion of the solution was weighed and mounted on a Mylar film.

The promethium samples were measured by a $5''\phi\times4''$ well-type NaI(Tl) scintillator with a 256-channel pulse height analyzer. An aluminum absorber of 6 mm in thickness was used to shield the $\beta$-rays. $^{147}$Pm, $^{148}$Pm, $^{149}$Pm, and $^{151}$Pm existed in the sample. As shown in **Fig. 1**, however, all $\gamma$-activities in the energy range higher than 1.26 MeV are due to $^{148g}$Pm and $^{148m}$Pm. The observed $\gamma$-activity in that energy region at time $t$ is given by Eq. (2).

$$A_{obs}=A_g^0[\varepsilon_g e^{-\lambda_g t}]+A_m^0\left[\varepsilon_m e^{-\lambda_m t}+\varepsilon_g\frac{k\cdot\lambda_g}{\lambda_g-\lambda_m}(e^{-\lambda_m t}-e^{-\lambda_g t})\right] \quad (2)$$

where the subscripts g and m stand for $^{148g}$Pm and $^{148m}$Pm, respectively, $A^0$ is the absolute decay rate at $t=0$, $\lambda$ is the decay constant, $\varepsilon$ is the counting efficiency, and k, 0.07, is the branching ratio for he isomeric transition of $^{148m}$Pm. In order to determine the counting efficiencies, standard $^{148}$Pm sources were prepared from a proton bombarded target of $^{148}$Nd enriched in 93%, and measured by $4\pi\beta$-counting. The losses due to the self-absorption in the $4\pi\beta$-counting were estimated to be less than 3% for $^{148m}$Pm and less than 1% for $^{148g}$Pm by $4\pi\beta$-$\gamma$ coincidence technique. By counting the standard sources the efficiencies were determined as follows; $\varepsilon_g=0.082\pm0.004$ and $\varepsilon_m=0.40\pm0.02$.

The other samples were measured by a $3''\phi\times3''$ NaI(Tl) with the pulse height analyzer. The absolute quantities of $^{137}$Cs, $^{60}$Co, and $^{54}$Mn were determined by comparing the counting rates of the main photopeaks with those of the respective standard sources whose accuracies of the absolute intensities were $\pm2\%$. The yield of $^{58}$Co was determined by counting the photopeak of the 808 KeV $\gamma$-ray whose efficiency was calibrated by the other standard sources. For the neodymium samples, it was necessary only to measure the relative intensity of $^{147}$Nd between the samples from uranium and neodymium targets.

## 2.4 Relation between uranium and neodymium targets

The nuclear transformation diagrams in the uranium and neodymium targets are considered as shown in **Fig. 2**. The dotted line represents the independent formation of $^{147}$Pm which is negligible compared with the cumulative yield of $^{147}$Nd. $^{147}$Nd may be considered as a direct product of fission, since the half-lives of its precursors are very short compared to that of $^{147}$Nd and to the irradiation period, and consequently the accumulation of $^{147}$Nd from its precursors has reached the equilibrium with the decay of $^{147}$Nd at the earlier stage of the irradiation.

The formations of $^{148m}$Pm and $^{148g}$Pm in the uranium target can be divided into the following terms.

$$N_m=N_{mf}+N_{mp}+N_{mn} \quad (3)$$

$$N_g=N_{gf}+N_{gmf}+N_{gp}+N_{gmp}+N_{gn}+N_{gmn} \quad (4)$$

where $N_m$ and $N_g$ are the total yields of $^{148m}$Pm and $^{148g}$Pm, $N_{mf}$ and $N_{gf}$ are the yields by fission, $N_{mp}$ and $N_{gp}$ are by neutron capture of $^{147}$Pm which is formed directly through fission, $N_{mn}$ and $N_{gn}$ are by neutron capture of $^{147}$Pm as the decay product of $^{147}$Nd. Finally $N_{gmf}$, $N_{gmp}$, and $N_{gmn}$ are the growths as a result of the isomeric transition of $^{148m}$Pm classified into three fractions corresponding to the three different types of the yields of $^{148m}$Pm, $N_{mf}$, $N_{mp}$, and $N_{mn}$, respectively.

In the neodymium target $^{148m}$Pm and $^{148g}$Pm are produced only by neutron capture of $^{147}$Pm formed by the decay of $^{147}$Nd. Then their yields can be written as Eqs. (5) and (6).

$$N'_m=N'_{mn} \quad (5)$$

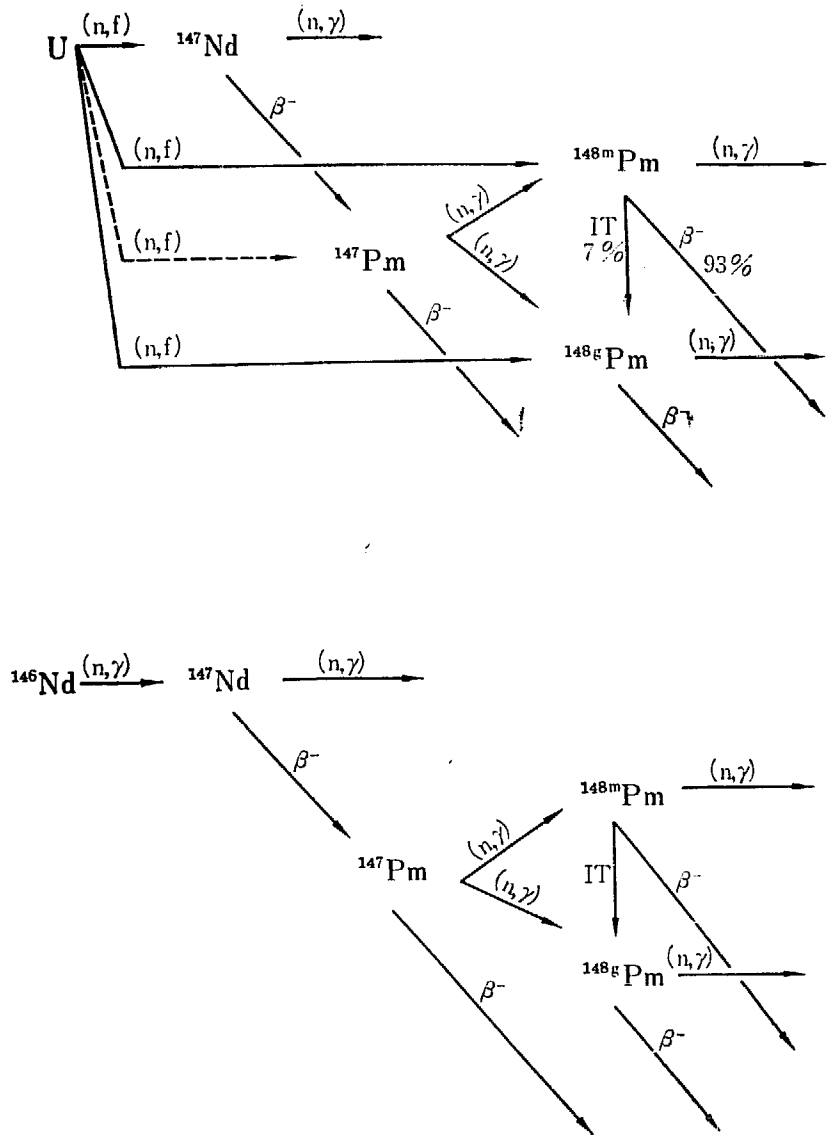


Fig. 2

$$N'_g = N'_{gn} + N'_{gmn} \quad (6)$$

Therefore if the uranium and neodymium targets are irradiated under the same conditions, the following relations hold.

$$\frac{N_{mn}}{N'_{mn}} = \frac{N_{gn}}{N'_{gn}} = \frac{N_{gmn}}{N'_{gmn}} = \frac{n_U \sigma_f y_{147}}{n_{Nd}\,\sigma_{Nd}} = \frac{N_{Nd}}{N'_{Nd}} \quad (7)$$

where $n_U$ is the number of uranium atoms, $n_{Nd}$ is that of $^{146}Nd$ atoms, $\sigma_f$ is the fission cross section of uranium, $\sigma_{Nd}$ is the (n, $\gamma$) reaction cross section of $^{146}Nd$, $y_{147}$ is the cummulative fission yield of $^{147}Nd$, and $N_{Nd}$ and $N'_{Nd}$ are the yields of $^{147}Nd$ in the uranium and neodymium target, respectively. Then the contributions of neutron capture of $^{147}Pm$ formed through $^{147}Nd$ are

$$N_{mn} = RN'_m \quad (8)$$

$$N_{gn} + N_{gmn} = RN'_g \quad (9),$$

where $R$ is the activity ratio of $^{147}Nd$ formed in the uranium target to that in the neodymium target.

## 3. Result and discussion

The results are shown in TABLE 1. The uncertainties of the data were estimated to be 10%

TABLE 1 Observed and subtractive values of $^{148m}$Pm and $^{148g}$Pm.

| Run | Target | $^{148m}$Pm (atoms) | | $^{148g}$Pm (atoms) | |
|---|---|---|---|---|---|
| | | observed | subtractive | observed | subtractive |
| I | $^{233}$U | $3.2\times10^{8}$ | $3.1\times10^{8}$ | $3.0\times10^{8}$ | $4.0\times10^{8}$ |
| II | $^{233}$U | $7.2\times10^{8}$ | $7.2\times10^{8}$ | $8.7\times10^{8}$ | $9.9\times10^{8}$ |
| III | $^{235}$U | $2.2\times10^{8}$ | $2.4\times10^{8}$ | $3.2\times10^{8}$ | $3.3\times10^{8}$ |
| IV | $^{235}$U | $3.0\times10^{9}$ | $3.0\times10^{9}$ | $3.8\times10^{9}$ | $3.4\times10^{9}$ |

as the standard deviation which was deduced from the standard deviations of 5% in the absolute counting, 5 % in the $\gamma$-counting, 1 % in the chemical yield, and 2—3 % in the decay constants. The total amounts of $^{148m}$Pm and $^{148g}$Pm observed in the uranium targets are equal within the experimental accuracy to the amounts of $^{148m}$Pm and $^{148g}$Pm to be subtracted from the observed values, respectively.

There are several possibilities of producing $^{148}$Pm in the neodymium target by other reactions than that shown in Fig. 2. None of them, however, could appreciablly contribute to form $^{148}$Pm. They are discussed as follows:

(1) $^{148}$Nd(n, $\gamma$)$^{149}$Nd $\xrightarrow{\beta^-,\ 1.8\,h}$ $^{149}$Pm(n, 2n)$^{148}$Pm

The threshold energy of the (n, 2n) reaction is 7.3 MeV. The reaction occurs only with fast neutrons. It was confirmed, by irradiating both natural neodymium and enriched $^{148}$Nd samples. that the formation of $^{148}$Pm depends on the abundance of $^{146}$Nd but does not depend on the abundance of $^{148}$Nd.

(2) $^{151}$Eu(n, $\alpha$)$^{148}$Pm

The reaction cross section is about 10 $\mu$b[13] for pile neutrons though the Q-value of the reaction is 7.7 MeV. Since the europium content was 3 ppm, this reaction should not produce more than 0.1% of the whole yield under the experimental conditions.

(3) $^{148}$Sm(n, p)$^{148}$Pm

The threshold energy is 1.7 MeV. This reaction also occurs only with fast neutrons. Furthermore, the proton emission may be reduced by the Coulomb barrier. The sammarium content was 30 ppm and the isotopic abundance of $^{148}$Sm is 11.2%. Therefore the contribution of this reaction may also be negligible.

(4) Presence of $^{147}$Pm as an impurity

It is not probable for $^{147}$Pm to exist in the neodymium target as an impurity. As mentioned in the paragraph of target preparation, the analysis of the neodymium sample showed there was no $\beta$-activity attributed to $^{147}$Pm.

(5) Contamination with uranium

No activities of fission products were detected in the irradiated neodymium target.

After all it should be concluded that $^{148m}$Pm and $^{148g}$Pm as the primary fission products were not detected in this experiment. However, 20% of the total amounts of observed $^{148}$Pm may be taken as the upper limit of that formed by fission, since the uncertainties of the data are $\pm$10%. To determine the upper limits, the results of run I and III were more sensitive to the limits.

The upper limits of the fractional independent yields of $^{148}$Pm were obtained as follows: The numbers of the atoms of $^{148m}$Pm, $^{148g}$Pm, and $^{137}$Cs at the end of the irradiation are given in Eqs. (10), (11), and (12), respectively.

$$N_{mf}=\frac{n_U \cdot y_m \cdot \sigma_f \cdot \Phi}{\Lambda_m}[1-\exp(-\Lambda_m t)] \tag{10}$$

$$N_{gf}+N_{gmf}=\frac{n_U \cdot y_g \cdot \sigma_f \cdot \Phi}{\Lambda_g}[1-\exp(-\Lambda_g t)] + \frac{k \cdot \lambda_m \cdot n_U \cdot y_m \cdot \sigma_f \cdot \Phi}{\Lambda_m}\left[\frac{1-\exp(-\Lambda_g t)}{\Lambda_g}-\frac{\exp(-\Lambda_m t)-\exp(-\Lambda_g t)}{\Lambda_g-\Lambda_m}\right] \tag{11}$$

$$N_{Cs}=\frac{n_U \cdot y_{Cs} \cdot \sigma_f \cdot \Phi}{\lambda_{Cs}}[1-\exp(-\lambda_{Cs}t)] \tag{12}$$

where $n_U$ is the number of uranium atoms, $\sigma_f$ is the fission cross section, $\Phi$ is the neutron flux, $y_m$, $y_g$, and $y_{Cs}$ are the fission yields of $^{148m}$Pm, $^{148g}$Pm, and $^{137}$Cs, respectively, $k$ is the branching ratio of the isomeric transition of $^{148m}$Pm, $t$ is the irradiation period, $\lambda_{Cs}$ is the decay constant of $^{137}$Cs, and $\Lambda_m$ and $\Lambda_g$ are the modified decay constants of $^{148g}$Pm and $^{148m}$Pm which are given by Eqs. (13) and (14).

$$\Lambda_m=\lambda_m+\sigma_m\Phi \tag{13}$$

$$\Lambda_g=\lambda_g+\sigma_g\Phi \tag{14}$$

where $\lambda_m$ and $\lambda_g$ are the decay constants and $\sigma_m$ and $\sigma_g$ are the neutron capture cross sections of $^{148m}$Pm and $^{148g}$Pm, respectively. Eqs. (10) and (11) are divided by Eq. (12) and $[1-\exp(\lambda_{Cs}t)]$ is approximated by $(\lambda_{Cs}t)$.

$$\frac{N_{mf}}{N_{Cs}}=\frac{y_m}{y_{Cs}}\left[\frac{1-\exp(-\Lambda_m t)}{\Lambda_m t}\right]$$

$$\frac{N_{gf}+N_{gmf}}{N_{Cs}}=\frac{y_g}{y_{Cs}}\left[\frac{1-\exp(-\Lambda_g t)}{\Lambda_g t}\right] \tag{15}$$

$$+\frac{y_m k\lambda_m}{y_{Cs}\Lambda_m t}\left[\frac{1-\exp(\Lambda_g t)}{\Lambda_g}-\frac{\exp(-\Lambda_m t)-\exp(-\Lambda_g t)}{\Lambda_g-\Lambda_m}\right] \tag{16}$$

Thus $y_m$ and $y_g$ were obtained from Eqs. (15) and (16) using the data in TABLE 2. The fractional independent yield is given by Eq. (17).

$$Y_{148}(\mathrm{Pm})=\frac{y_m+y_g}{y_{148}} \tag{17}$$

where $y_{148}$ is the total chain yield of mass number 148.

TABLE 2 Numerical values used in the calculation of the fractional independent yields.

| Nuclear data | | Experimental data | | |
|---|---|---|---|---|
| $\lambda_m$ | 0.0161 day$^{-1}$[14] | Run | I | II |
| $\lambda_g$ | 0.128 day$^{-1}$[14] | $N_{mf}$ (atoms) | $\lesssim 6.4\times10^{7}$ | $\lesssim 4.4\times10^{7}$ |
| $\sigma_m$ | $3\times10^{4}$ barns[11] | $N_{gf}+N_{gmf}$ (atoms) | $\lesssim 7.2\times10^{7}$ | $\lesssim 6.4\times10^{7}$ |
| $\sigma_g$ | $3\times10^{3}$ barns[11] | $N_{Cs}$ (atoms) | $9.55\times10^{13}$ | $1.26\times10^{14}$ |
| $k$ | 0.07[4] | $\Phi$ (cm$^{-2}$·day$^{-1}$) | $8.6\times10^{17}$ | $9.5\times10^{17}$ |
| $y_{Cs}$ | 6.58% for $^{233}$U[14] | $t$ (days) | 4.17 | 2.47 |
| | 6.15% for $^{235}$U[14] | | | |
| $y_{148}$ | 1.34% for $^{233}$U[14] | | | |
| | 1.71% for $^{235}$U[14] | | | |

TABLE 3 Observed and expected values of the fractional independent yields of $^{148}$Pm and the most probable charges of mass 148.

| Target | $^{233}$U | $^{235}$U |
|---|---|---|
| Fractional independent yields | | |
| observed | $\lesssim 8.5\times10^{-6}$ | $\lesssim 3.5\times10^{-6}$ |
| calculated with $c=0.94$ | $1.3\times10^{-3}$ | $7.5\times10^{-5}$ |
| $c=0.79$ | $4.5\times10^{-4}$ | $1.5\times10^{-5}$ |
| Most probable charges | | |
| observed | $\lesssim 57.8$ | $\lesssim 57.7$ |
| calculated by Wahl's function | 58.6 | 58.1 |
| by ECD rule | 58.7 | 58.2 |

The upper limits obtained are shown in TABLE 3. They are too small compared with the expected values that were obtained by the WAHL's $Z_p$ values and the charge distribution curve of Eq. (1)[1]. The data of the neutron capture cross sections of $^{148m}$Pm and $^{148g}$Pm are not accurate[11]. The fractional independent yields may be affected by a factor of 2 although the

capture cross sections are changed by a factor of 10.

Similar discrepancies have been observed for the yields of $^{96}$Nb and $^{97}$Nb in thermal neutron fission of $^{235}$U and $^{233}$U, for the yields of $^{136}$Xe in thermal neutron fission of $^{235}$U, $^{233}$U, and $^{239}$Pu, and for the yields of $^{86}$Rb in thermal neutron fission of $^{233}$U and $^{239}$Pu[1]. These cases were discussed in connection with the shell effects. Both $^{148}$Pm and its complementary fragment, however, are quite far from any shell edges.

Assuming that the charge distribution curve given by Eq. (1) with $c=0.94$ is applicable to the fission product chain of mass 148, the upper limits of $Z_p$ values were estimated. As shown in TABLE 3, they are smaller than the values expected either from the WAHL's function[1] or the equal charge displacement hypothesis.[3] The limits of $Z_p$ are 58.0 for $^{233}$U and 57.9 for $^{235}$U if $c=0.79$ is taken. There is still a large difference for $^{233}$U. These small $Z_p$ values eventually agree in their tendency with the result of Armbruster et al.,[15] whose $Z_p$ values were obtained by physical measurements and agreed neither with the WAHL's function nor with the equal charge displacement rule.

On the other hand, the fractional independent yield of $^{150}$Pm in the thermal neutron fission of $^{235}$U was reported by CHU[16] as $(2.1\pm0.1)\times10^{-3}$ which agrees well with the WAHL's formulation. However, it was determined by the mass spectrometry of $^{150}$Sm which was mostly attributed to the yield of $^{150}$Pm. Therefore there remains a little question about the formation of $^{150}$Sm by neutron capture of $^{149}$Sm which has a very large capture cross section.

## Acknowledgments

The auther expresses his appreciation to Dr. H. NATSUME, Dr. E. TAKEKOSHI, and Dr. H. AMANO for their suggestions.

The kind guidance and assistance by Dr. T. WATANABE of Nagoya University for the absolute measurement are greatly appreciated.

He also thanks Mrs. V. MIHAILOVA, a guest from the Institute of Physics, Bulgarian Academy of Science, for her assistance during part of the experiment, and Mr. K. OKAMOTO and Dr. H. BABA for their revision of the manuscript.

## References

1) A. C. WAHL, R. L. FERGUSON, D. R. NETHAWAY, D. E. TROUTNER, and K. WOLFSBERG: *Phys. Rev.* **126**, 1112-1126 (1962).
2) E. K. HYDE; The Nuclear Properties of the Heavy Elements III, Capter 5, 141-156, Prentice-Hall, Inc., Englewood Cliffs, New Jersey (1964).
3) GLENDENIN, CORYELL, and EDWARDS: Paper 52 in "Radiochemical Studies: The Fission Products," C. D. CORYELL and N. SUGARMAN, editors, Nat. Nucl. Energ. Ser., Plutonium Project Record, McGraw-Hill Book Co., Inc., New York (1951).
4) Nuclear Data Sheets, National Research Council, 61-4-51, Washington D.C.(1961)
5) C. V. K. BABA, G. T. EWAN, and J. F. SUAREZ: *Nuclear Phys.*, **43**, 264-284 (1963).
6) J. R. HUIZENGA and R. VANDENBOSCH: *Phys. Rev.*, **120**, 1305-1312 (1960).
7) R. VANDENBOSCH and J. R. HUIZENGA: *Phys. Rev.*, **120**, 1313-1318 (1960).
8) I. F. CROALL and H. H. WILLIS: *J. Inorg. Nucl. Chem.*, **24**, 221-227 (1962).
9) D.G. SARANTITES, G.E. GORDEN, and C.D. CORYELL: *Phys. Rev.*, **138**, B 353-364 (1965).
10) G. B. COOK: results cited in paper: A. C. Pappas, Proceedings of the International Conference on the Peaceful Uses of Atomic Energy **7**, 3-14, United Nations (1956).
11) R. P. SCHUMAN and J. R. BERRETH: *Nucl. Sci. Eng.*, **12**, 519-522 (1962).
12) R. KO: Nucleonics, **15**, No. 1, 72-77 (1957).
13) H. UMEZAWA and K. OKAMOTO: unpublished.
14) S. KATCOFF: *Nucleonics*, **18**, No. 11, 201-208 (1960).
15) P. ARMBRUSTER, D. HOVESTADT, H. MEISTER, and H. J. SPECHT: *Nuclear Phys.*, **54**, 586-614 (1964).
16) Y. Y. CHU: UCRL-8926 (1959).

## Appendix

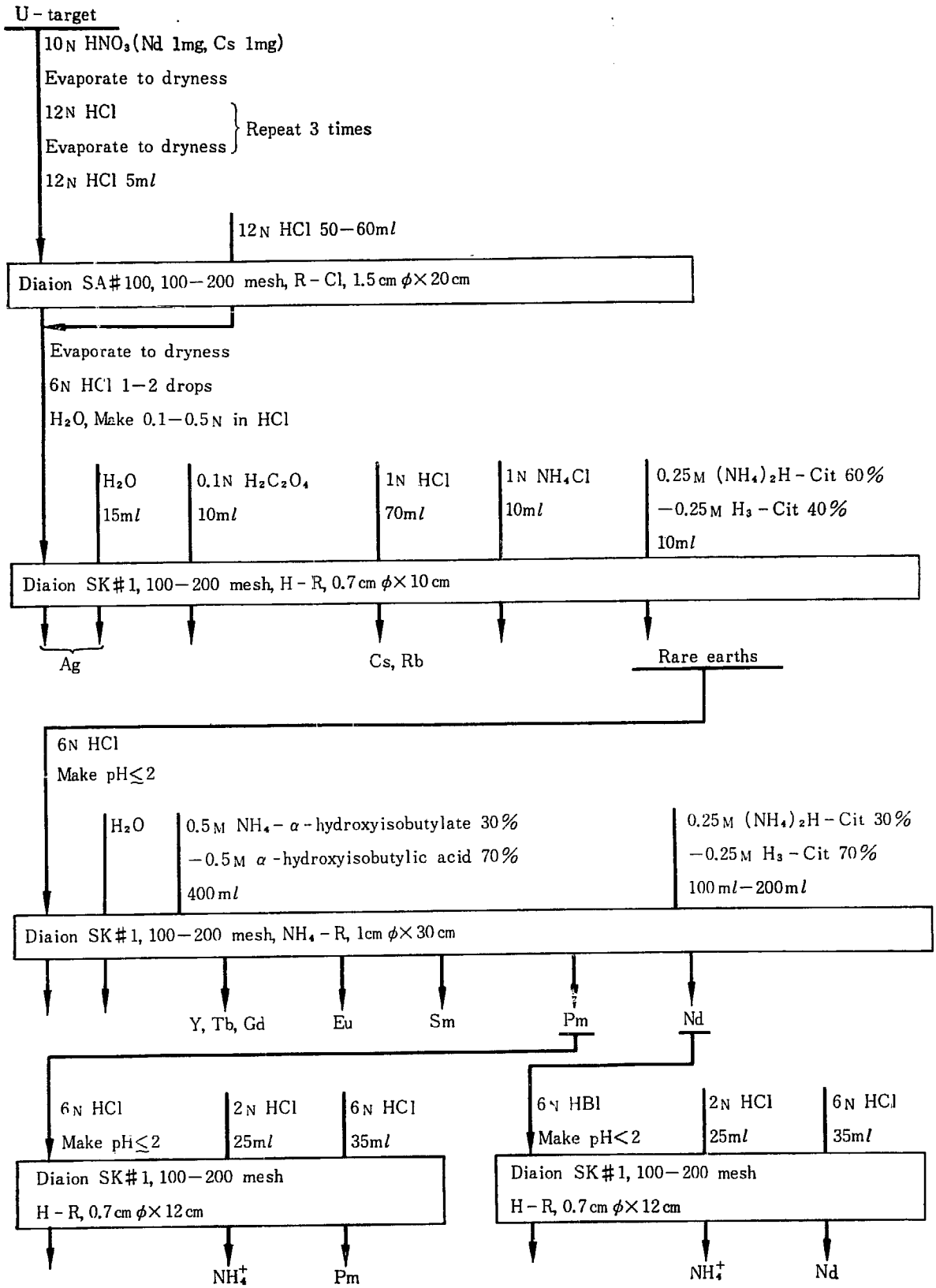


**Fig. 3** Separation scheme.

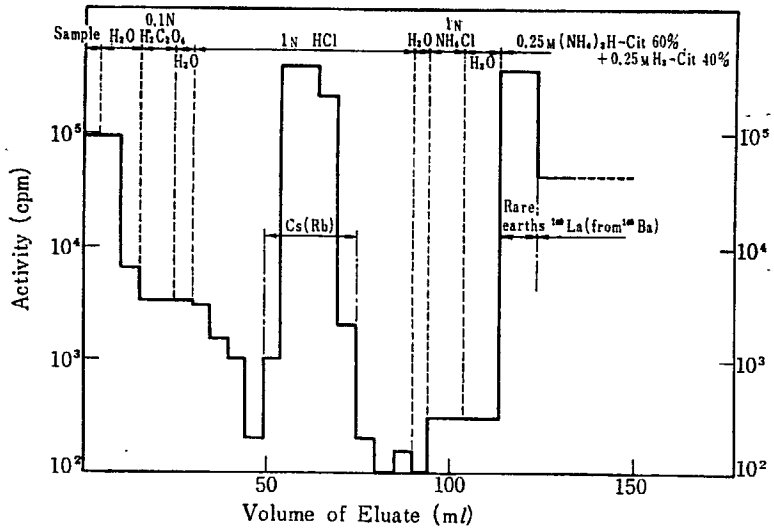


**Fig. 4** Elution Curve of Cesium and gross Rear earth elements

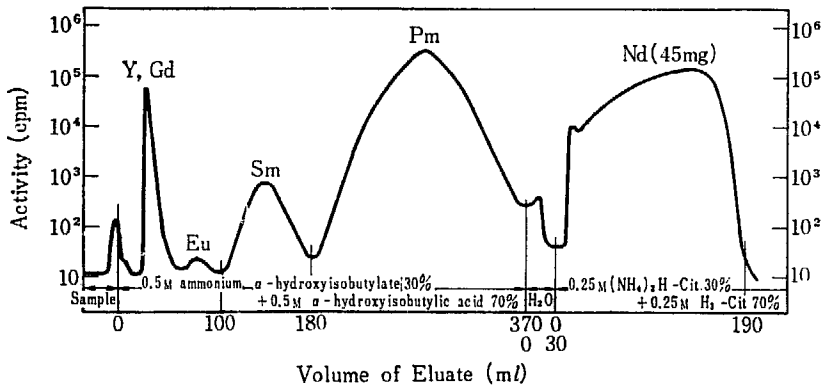


**Fig. 5** Elution curve of Rear-earth elments